

Препринти Інституту фізики конденсованих систем НАН України розповсюджуються серед наукових та інформаційних установ. Вони також доступні по електронній комп'ютерній мережі на WWW-сервері інституту за адресою <http://www.icmp.lviv.ua/>

The preprints of the Institute for Condensed Matter Physics of the National Academy of Sciences of Ukraine are distributed to scientific and informational institutions. They also are available by computer network from Institute's WWW server (<http://www.icmp.lviv.ua/>)

Оксана Вадимівна Пацаган

ФАЗОВЕ СПІВІСНУВАННЯ ГАЗ-РІДИНА В БІНАРНИХ ІОННИХ ПЛИНАХ
З ЕКРАНОВАНИМИ КУЛОНІВСЬКИМИ ВЗАЄМОДІЯМИ. ВПЛИВ
РАДІУСА ВЗАЄМОДІЇ НА ТЕМПЕРАТУРУ КРОССОВЕРА

Роботу отримано 27 грудня 2013 р.

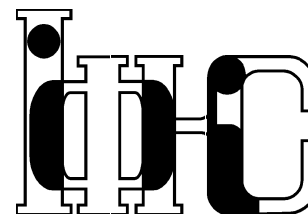
Затверджено до друку Вченою радою ІФКС НАН України

Рекомендовано до друку відділом квантово-статистичної теорії
процесів каталізу

Виготовлено при ІФКС НАН України

© Усі права застережені

Національна академія наук України



ІНСТИТУТ
ФІЗИКИ
КОНДЕНСОВАНИХ
СИСТЕМ

ICMP-13-09E

O.V. Patsahan

GAS-LIQUID PHASE COEXISTENCE IN BINARY IONIC
FLUIDS WITH SCREENED COULOMB INTERACTIONS.
THE EFFECT OF AN INTERACTION RANGE
ON THE CROSSOVER TEMPERATURE

ЛЬВІВ

УДК: 538.9

PACS: 05.70.Fh, 64.60.De, 64.60.F-

Фазове співіснування газ-рідина в бінарних іонних плинах з екранованими кулонівськими взаємодіями. Вплив радіуса взаємодії на температуру кроссовера

О.В. Пацаган

Анотація. Досліджується фазова діаграма газ-рідина і температура кроссовера модельного бінарного плину, в якому частинки з твердим кором взаємодіють за допомогою екранованих кулонівських потенціалів з оберненим радіусом екранування z таким чином, що однакові сорти відштовхуються, а різні сорти притягуються. Показано в рамках теорії середнього поля, що область, в якій співіснують газова і рідка фази, зменшується з ростом z і зовсім зникає при $z \approx 3$. Отримані результати якісно узгоджуються з результатами комп'ютерних симуляцій. Також показано, що збільшення радіуса взаємодії веде до зменшення температури кроссовера. Для $z \leq 0.05$, температура кроссовера стає такою ж як для обмеженої примітивної моделі.

Gas-liquid phase coexistence in binary ionic fluids with screened Coulomb interactions. The effect of an interaction range on the crossover temperature

O.V. Patsahan

Abstract. We study the gas-liquid phase diagram and the crossover temperature of a model binary fluid in which hard-core particles interact via screened Coulomb potentials with the inverse screening length z : like particles repel each other and unlike particles attract (YRPM). Using the mean-field theory we find that the gas-liquid coexistence region reduces with an increase of z and completely vanishes at $z \approx 3$. This is in qualitative agreement with the simulation findings. It is also shown that an increase in the interaction range leads to the decrease of the crossover temperature. For $z \leq 0.05$, the crossover temperature is the same as for the restricted primitive model.

Подається в Condensed Matter Physics

Submitted to Condensed Matter Physics

© Інститут фізики конденсованих систем 2013
Institute for Condensed Matter Physics 2013

1. Introduction

The nature of criticality in ionic fluids with the dominant Coulomb interactions has been an outstanding experimental and theoretical issue for many years. Now, a generally accepted idea is that the phase transition in these systems belongs to the universal class of a tree-dimensional Ising model [1–10]. Nevertheless, the crossover from the mean-field-like behaviour to the Ising model criticality when approaching the critical point remains a challenging problem for theory, simulations and experiments [3].

Quite recently, we have developed the theory that allows one to derive all the relevant coefficients of the Landau-Ginzburg (LG) Hamiltonian within the framework of the same approximation [11]. The Ginzburg temperature for a purely Coulombic model calculated using this theory turned out to be about 20 times smaller than for a nonionic model. We have also considered the model which, besides Coulomb interactions, includes short-range attractive interactions. For this model, we have found a decrease of the reduced crossover temperature with a decrease of a solvent dielectric constant [11], which agrees with the available experimental observations [3].

In the present work, we extend our previous investigations to the study of the gas-liquid phase behavior and the crossover temperature in binary ionic fluids with screened Coulomb interactions. Specifically, we consider a two-component system of particles labeled 1 and 2, such that the interaction potential between a particle of species α and one of the species β at a distance r apart is

$$u_{\alpha\beta}(r) = \begin{cases} \infty, & r < \sigma \\ (-1)^{\alpha+\beta} K \frac{\exp(-z(r/\sigma - 1))}{r/\sigma}, & r \geq \sigma \end{cases}, \quad (1.1)$$

where $\alpha, \beta = (1, 2)$. For $K > 0$, Eq. (1.1) describes a symmetrical mixture of hard spheres of diameter σ in which the like particles interact through a repulsive Yukawa potential for $r > \sigma$, and the unlike particles interact through the opposite attractive Yukawa potential for $r > \sigma$. We restrict our consideration to the case where the number densities of species 1 and 2 are the same, i.e., $\rho_1 = \rho_2 = \rho/2$. For $K = (Ze)^2/\epsilon$, the model (1.1) is called a Yukawa restricted primitive model (YRPM). In the limit $z \rightarrow \infty$, the YRPM reduces to a hard sphere model whereas the RPM is recovered by taking the limit $z \rightarrow 0$.

It is worth noting that the YRPM model is often used to model the system of oppositely charged colloids [12–15]. The effective (screened)

colloid-colloid interactions in such a system are due to the presence of co- and counter-ions in the solvent. In this case, K and z take the form: $K/k_B T = Z^2 \lambda_B / (1 + \kappa_D \sigma / 2)^2 / \sigma$ and $z = \kappa_D \sigma$, where $\kappa_D = \sqrt{8\pi \lambda_B \rho_s}$ is the inverse Debye screening length, $\lambda_B = e^2 / \epsilon_s k_B T$ is the Bjerrum length, ρ_s is the salt concentration and ϵ_s is the dielectric constant of the solvent. In a colloid system, the range of interaction can be modified by changing the salt concentration.

Extensive simulations of the YRPM predict a rich phase diagram involving a gas-liquid phase separation as well as several crystalline phases which is in agreement with experimental confocal microscopy data [12–15]. These studies indicate a sensitivity of the phase diagram to the variation of z . In particular, it is found that the gas-liquid separation is stable with respect to gas-solid coexistence for $z \leq 4$ [14].

The gas-liquid phase transition in the YRPM was studied theoretically using the generalized mean-spherical approximation (GMSA) [16] and the hierarchical reference theory (HRT) [10]. The results obtained from the GMSA show that both the critical density and the critical temperature increase above the corresponding values for the RPM when z increases (up to $z \approx 4$). Moreover, the GMSA predicts a non-monotonous behavior of the critical temperature as a function of z . In Ref. [10] the main emphasis is made on the critical behavior of the YRPM including the limiting case $z \rightarrow 0$.

In this paper, using the theory developed in Ref. [11], we study the effects of the interaction range on the gas-liquid phase diagram of the YRPM. Our discussion also involves an analysis of the dependence of the crossover temperature on the interaction range.

2. Theory

2.1. Functional representation of the grand partition function

Using the Weeks-Chandler-Andersen (WCA) regularization scheme [17] for the Yukawa potential inside the hard core, we rewrite the interaction potential (1.1) as follows:

$$u_{\alpha\beta}(r) = \phi^{\text{HS}}(r) + \phi_{\alpha\alpha}^Y(r), \quad (2.1)$$

where $\phi^{\text{HS}}(r)$ is the interaction potential between the two hard spheres of diameter σ

$$\phi^{\text{HS}}(r) = \begin{cases} \infty, & r < \sigma \\ 0, & r \geq \sigma \end{cases}, \quad (2.2)$$

and $\phi_{\alpha\beta}^Y(r)$ has the form:

$$\phi_{\alpha\beta}^Y(r) = \begin{cases} (-1)^{\alpha+\beta} K, & r < \sigma \\ (-1)^{\alpha+\beta} K \frac{\exp(-z(r/\sigma - 1))}{r/\sigma}, & r \geq \sigma \end{cases}, \quad \alpha, \beta = (1, 2). \quad (2.3)$$

Thermodynamic and structural properties of the system interacting through the potential $\phi^{\text{HS}}(r)$ are assumed to be known. Therefore, the one-component hard-sphere model is regarded as the reference system.

The model under consideration is at equilibrium in the grand canonical ensemble, $\beta = (k_B T)^{-1}$ is the inverse temperature, $\nu_\alpha = \beta \mu_\alpha$ ($\nu_\alpha = \nu_\beta = \nu$) is the dimensionless chemical potential of the α th species. Using the CV method we present the grand partition function (GPF) of the model in the form of a functional integral [11, 18]:

$$\begin{aligned} \Xi[\nu_\alpha] = & \Xi_{\text{HS}} \exp(\Delta \nu_N \langle N \rangle_{\text{HS}}) \int (d\rho)(d\omega) \exp(\Delta \nu_N \rho_{0,N} \\ & - \frac{\beta}{2V} \sum_{\mathbf{k}} \tilde{\phi}^Y(k) \rho_{\mathbf{k},C} \rho_{-\mathbf{k},C} + i \sum_{\mathbf{k}} (\omega_{\mathbf{k},N} \rho_{\mathbf{k},N} + \omega_{\mathbf{k},C} \rho_{\mathbf{k},C}) \\ & + \sum_{n \geq 2} \frac{(-i)^n}{n!} \sum_{i_n \geq 0} \sum_{\mathbf{k}_1, \dots, \mathbf{k}_n} \mathfrak{M}_n^{(i_n)}(k_1, \dots, k_n) \omega_{\mathbf{k}_1, C} \dots \omega_{\mathbf{k}_{i_n}, C} \\ & \times \omega_{\mathbf{k}_{i_n+1}, N} \dots \omega_{\mathbf{k}_n, N} \delta_{\mathbf{k}_1 + \dots + \mathbf{k}_n}), \end{aligned} \quad (2.4)$$

Here, the following notations are introduced. Ξ_{HS} is the GPF of the one-component hard-sphere model with the dimensional chemical potential ν_{HS} . Hereafter, the subscript HS refers to the hard-sphere system. $\Delta \nu_N = \bar{\nu} - \nu_{\text{HS}}$ where

$$\bar{\nu} = \bar{\nu}_\alpha = \nu_\alpha + \frac{\beta}{2V} \sum_{\mathbf{k}} \tilde{\phi}_{\alpha\alpha}^Y(k), \quad \alpha = (1, 2). \quad (2.5)$$

$\tilde{\phi}_{\alpha\beta}^Y(k)$ is the Fourier transform of the repulsive potential

$$\phi^Y(r) = K \sigma \exp[-z(r/\sigma - 1)]/r.$$

In the case of the WCA regularization, $\beta \tilde{\phi}^Y(k)$ has the form

$$\beta \tilde{\phi}^Y(x) = \frac{4\pi\sigma^3}{T^* x^3 (z^2 + x^2)} \left\{ [z^2 + x^2(1+z)] \sin(x) - xz^2 \cos(x) \right\}, \quad (2.6)$$

where $T^* = (\beta K)^{-1}$ is the reduced temperature and $x = k\sigma$.

$\rho_{\mathbf{k},N}$ and $\rho_{\mathbf{k},C}$ are the CVs which describe fluctuations of the total number density and the relative number density (or concentration), respectively:

$$\rho_{\mathbf{k},N} = \rho_{\mathbf{k},+} + \rho_{\mathbf{k},-}, \quad \rho_{\mathbf{k},C} = \rho_{\mathbf{k},+} - \rho_{\mathbf{k},-},$$

CV $\rho_{\mathbf{k},\alpha} = \rho_{\mathbf{k},\alpha}^c - i\rho_{\mathbf{k},\alpha}^s$ describes the value of the \mathbf{k} -th fluctuation mode of the number density of the α th species, the indices c and s denote real and imaginary parts of $\rho_{\mathbf{k},\alpha}$; CVs ω_N and ω_C are conjugate to ρ_N and ρ_C , respectively. $(d\rho)$ and $(d\omega)$ denote volume elements of the CV phase space:

$$(d\rho) = \prod_{A=N,C} d\rho_{0,A} \prod_{\mathbf{k} \neq 0}' d\rho_{\mathbf{k},A}^c d\rho_{\mathbf{k},A}^s,$$

$$(d\omega) = \prod_{A=N,C} d\omega_{0,A} \prod_{\mathbf{k} \neq 0}' d\omega_{\mathbf{k},A}^c d\omega_{\mathbf{k},A}^s,$$

and the product over \mathbf{k} is performed in the upper semi-space ($\rho_{-\mathbf{k},A} = \rho_{\mathbf{k},A}^*$, $\omega_{-\mathbf{k},A} = \omega_{\mathbf{k},A}^*$).

The n th cumulant $\mathfrak{M}_n^{(in)}$ is a linear combination of the initial cumulants $\mathfrak{M}_{\alpha_1 \dots \alpha_n}$ which, in turn, coincide with the Fourier transforms of the partial connected correlation functions of the hard-sphere system. We have the following recurrence relations for the cumulants [18]:

$$\begin{aligned} \mathfrak{M}_n^{(0)} &= \tilde{G}_{n,HS}, & \mathfrak{M}_n^{(1)} &= 0, \\ \mathfrak{M}_n^{(2)} &= \tilde{G}_{n-1,HS}, & \mathfrak{M}_n^{(3)} &= 0, \\ \mathfrak{M}_n^{(4)} &= 3\tilde{G}_{n-2,HS} - 2\tilde{G}_{n-1,HS}, \end{aligned}$$

where $\tilde{G}_{n,HS}(k)$ is the Fourier transform of the n -particle connected correlation function of a one-component hard-sphere system.

2.2. Effective Ginzburg-Landau Hamiltonian

We consider the model (2.3) near the gas-liquid critical point. In this case, the phase space of CVs $\rho_{\mathbf{k},N}$ contains CV $\rho_{0,N}$ related to the order parameter. In order to obtain the effective Hamiltonian in terms of $\rho_{\mathbf{k},N}$ one should integrate out CVs $\rho_{\mathbf{k},C}$ and $\omega_{\mathbf{k},C}$. The detailed derivation of such type of Hamiltonian is given in Ref. [11]. Using the results of Ref. [11], we can write the expression for the effective φ^4 LG Hamiltonian

of the model under consideration

$$\begin{aligned} \mathcal{H}^{eff} &= a_{1,0}\rho_{0,N} + \frac{1}{2!\langle N \rangle} \sum_{\mathbf{k}} (a_{2,0} + k^2 a_{2,2}) \rho_{\mathbf{k},N} \rho_{-\mathbf{k},N} \\ &+ \frac{1}{3!\langle N \rangle^2} \sum_{\mathbf{k}_1, \mathbf{k}_2} a_{3,0} \rho_{\mathbf{k}_1,N} \rho_{\mathbf{k}_2,N} \rho_{-\mathbf{k}_1 - \mathbf{k}_2,N} \\ &+ \frac{1}{4!\langle N \rangle^3} \sum_{\mathbf{k}_1, \mathbf{k}_2, \mathbf{k}_3} a_{4,0} \rho_{\mathbf{k}_1,N} \rho_{\mathbf{k}_2,N} \rho_{\mathbf{k}_3,N} \rho_{-\mathbf{k}_1 - \mathbf{k}_2 - \mathbf{k}_3,N}, \end{aligned} \quad (2.7)$$

with the coefficients having the following form in a one-loop approximation:

$$a_{1,0} = -\Delta\nu_N - \tilde{\mathcal{C}}_{1,Y} \quad (2.8)$$

$$a_{n,0} = -\rho^{n-1} \tilde{\mathcal{C}}_{n,HS} - \rho^{n-1} \tilde{\mathcal{C}}_{n,Y} \quad (2.9)$$

$$a_{2,2} = -\frac{1}{2} \rho \tilde{\mathcal{C}}_{2,HS}^{(2)} - \frac{1}{4\langle N \rangle} \sum_{\mathbf{q}} \tilde{g}^{(2)}(\mathbf{q}) [1 + \tilde{g}(\mathbf{q})]. \quad (2.10)$$

Here, we introduce the following notations. The superscript (2) in Eq. (2.10) denotes the second-order derivative with respect to the wave vector. $\tilde{\mathcal{C}}_{n,HS}$ is the Fourier transform of the n -particle direct correlation function of a one-component hard-sphere system in the long-wavelength limit. Explicit expressions for $\tilde{\mathcal{C}}_{n,HS}$ and $\tilde{\mathcal{C}}_{2,HS}^{(2)}$ for $n \leq 4$ in the Percus Yevick approximation are given in Ref. [11].

The term $\rho^{n-1} \tilde{\mathcal{C}}_{n,Y}$ denotes the contribution resulting from the integration over CVs $\rho_{\mathbf{k},C}$ and $\omega_{\mathbf{k},C}$

$$\rho^{n-1} \tilde{\mathcal{C}}_{n,Y} = \frac{(n-1)!}{2} \frac{1}{\langle N \rangle} \sum_{\mathbf{q}} [\tilde{g}(\mathbf{q})]^n, \quad (2.11)$$

$$\tilde{g}(\mathbf{q}) = -\frac{\beta \rho \tilde{\phi}^Y(\mathbf{q})}{1 + \beta \rho \tilde{\phi}^Y(\mathbf{q})}. \quad (2.12)$$

Taking into account Eq. (2.6) and (2.12), we obtain the following explicit expressions for $\rho^{n-1} \tilde{\mathcal{C}}_{n,Y}$:

$$\begin{aligned} -\rho^{n-1} \tilde{\mathcal{C}}_{n,Y} &= \frac{(n-1)!(-24\eta)^{n-1}}{\pi} \int_0^\infty dx x^2 \\ &\times \left[\frac{\tilde{f}(x)}{T^* x^3 (z^2 + x^2) + 24\eta f(x)} \right]^n, \end{aligned} \quad (2.13)$$

where

$$\tilde{f}(x) = [z^2 + x^2(1+z)] \sin(x) - xz^2 \cos(x) \quad (2.14)$$

and $\eta = \pi\rho\sigma^3/6$ is the packing fraction. $\Delta\nu_N$ is given by Eq. (2.5) and can be rewritten as follows:

$$\Delta\nu_N = \nu - \nu_{\text{HS}} + \frac{1}{2T^*}, \quad (2.15)$$

Summarizing, the expressions for coefficients $a_{n,0}$ for $n \geq 2$ and $a_{2,2}$ consist of two terms. While the first term depends solely on the characteristics of a hard-sphere system, the second term is of mixed type and takes into account the concentration-concentration (or charge-charge) correlations. Coefficient $a_{1,0}$ is the excess part of the chemical potential ν , and the equation $a_{1,0} = 0$ gives the chemical potential in the random phase approximation. Using Eqs. (2.8), (2.13) and (2.15), one obtains for ν

$$\nu = \nu_{\text{HS}} - \frac{1}{2T^*} + \frac{1}{\pi} \int_0^\infty \frac{x^2 \bar{f}(x)}{T^* x^3 (z^2 + x^2) + 24\eta \bar{f}(x)} dx \quad (2.16)$$

Coefficient $a_{2,2}$ describes the square-gradient term. The explicit expression for $a_{2,2}$ is too long to be presented herein.

3. Gas-liquid phase transition

In this section we study the gas-liquid phase diagram of the model (2.1) using Eqs. (2.8)-(2.16). First, we present the coefficient $a_{2,0}$ as $a_{2,0} = \bar{a}_{2,0} + a_{2,t}t$, where $\bar{a}_{2,0} = a_{2,0}(t=0)$, $a_{2,t} = \partial a_{2,0}/\partial t|_{t=0}$, and $t = (T - T_c)/T_c$. Hereafter, the subscript c refers to the critical value.

Taking into account Eqs. (2.9) and (2.13), we obtain for $a_{2,t}$

$$a_{2,t} = \frac{48\eta T_c^*}{\pi} \int_0^\infty \frac{x^5 (z^2 + x^2) \bar{f}^2(x)}{(T^* x^3 (z^2 + x^2) + 24\eta \bar{f}(x))^3} dx, \quad (3.1)$$

where \bar{f} is given by (2.14).

At the critical point, the system of equations

$$\bar{a}_{2,0}(\rho_c, T_c) = 0, \quad a_{3,0}(\rho_c, T_c) = 0 \quad (3.2)$$

holds yielding the critical temperature and the critical density. These equations, using Eqs. (2.9) and (2.13), can be rewritten in the form:

$$\frac{(1+2\eta)^2}{(1-\eta)^4} - \frac{24\eta}{\pi} \int_0^\infty \frac{x^2 \bar{f}^2(x) dx}{[T^* x^3 (z^2 + x^2) + 24\eta \bar{f}(x)]^2} = 0 \quad (3.3)$$

$$\frac{(1-7\eta-6\eta^2)(1+2\eta)}{(1-\eta)^5} - \frac{1152\eta^2}{\pi} \int_0^\infty \frac{x^2 \bar{f}^3(x) dx}{[T^* x^3 (z^2 + x^2) + 24\eta \bar{f}(x)]^3} = 0, \quad (3.4)$$

where the PY approximation is used for $\tilde{\mathcal{C}}_{n,\text{HS}}$.

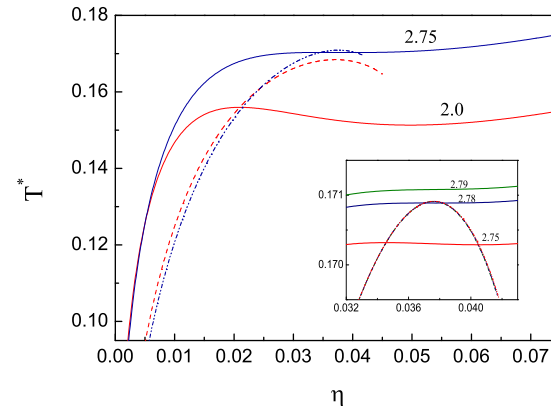


Figure 1. The loci of equations $\bar{a}_2 = 0, 0$ (solid lines) and $a_{3,0} = 0$ (dashed line) for $z = 2$ and $z = 2.75$. The cases $z = 2.75$, $z = 2.78$ and $z = 2.79$ are depicted at the inset.

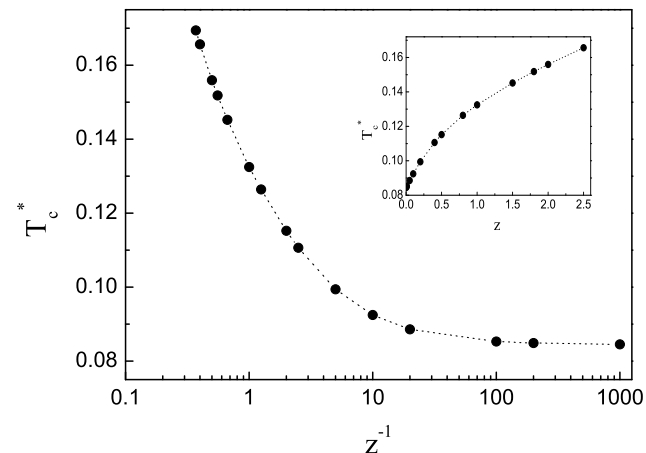


Figure 2. The reduced critical temperature of the YRPM as a function of the interaction range. The inset shows T_c^* as a function of z . The line is guide to the eye.

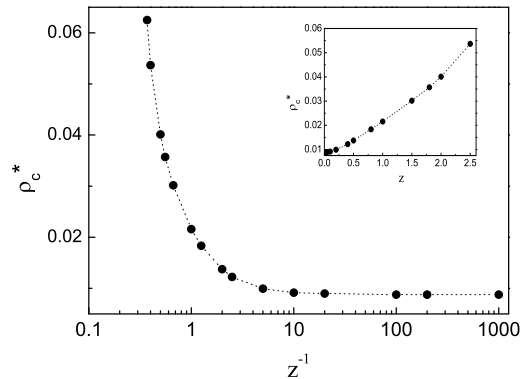


Figure 3. The reduced critical density of the YRPM as a function of the interaction range. The inset shows ρ_c^* as a function of z . The line is guide to the eye.

Table 1. The reduced gas-liquid critical parameters, the coefficients of the effective Hamiltonian and the reduced Ginzburg temperature t_G depending on the dimensionless inverse screening length for the Yukawa-RPM model (see the text) in the one-loop approximation.

z	T_c^*	ρ_c^*	$a_{2,t}$	$a_{2,2}$	$a_{4,0}$	t_G
2.78	0.170886	0.0707	1.7322	0.1750	0.0152	$8 * 10^{-5}$
2.77	0.170697	0.0684	1.7035	0.1750	0.0434	0.0007
2.75	0.170319	0.0661	1.675	0.173	0.0695	0.0018
2.7	0.169384	0.0625	1.6307	0.1699	0.1076	0.0046
2.6	0.167523	0.0573	1.5699	0.166	0.1576	0.0109
2.5	0.165656	0.0535	1.5258	0.1635	0.1901	0.0171
2.0	0.155964	0.0400	1.3778	0.1580	0.2784	0.0452
1.8	0.15183	0.0357	1.3333	0.1577	0.2986	0.0540
1.5	0.145215	0.0301	1.2750	0.1594	0.3109	0.0592
1	0.13248	0.0215	1.1910	0.1702	0.3064	0.0506
0.8	0.126383	0.0182	1.161	0.1793	0.2939	0.0409
0.5	0.11521	0.0138	1.1184	0.202	0.2508	0.0216
0.4	0.110640	0.0122	1.1069	0.2135	0.2394	0.0168
0.1	0.09245	0.0091	1.0784	0.2521	0.1816	0.0060
0.05	0.08857	0.0089	1.0762	0.2555	0.1756	0.0054
0.01	0.0853	0.0088	1.0759	0.257	0.1754	0.0053
0.005	0.08488	0.0088	1.0758	0.257	0.1752	0.0053
0.001	0.08454	0.0088	1.0758	0.257	0.1752	0.0053

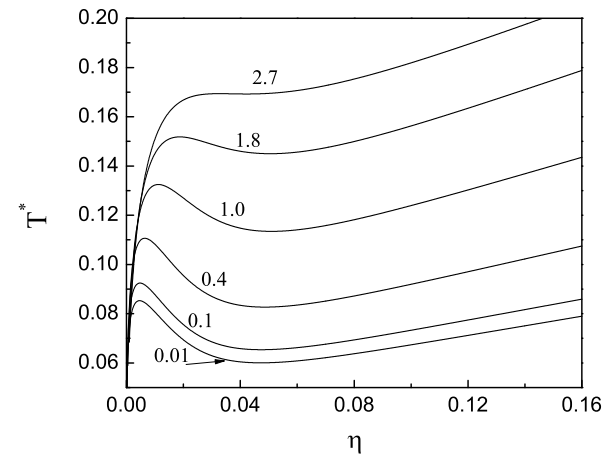


Figure 4. The spinodal curves of the YRPM for different values of z .

Solving Eqs. (3.3)-(3.4) we obtain the critical temperature and the critical density for z ranging from $z = 0.001$ to $z = 2.78$. At $z = 2.79$, the system of equations (3.3)-(3.4) has no solution in the region of the gas-liquid phase transition (see Fig. 1). The results for critical parameters for different values of z are presented in Table 1. The dependence of T_c^* and ρ_c^* on the parameter z^{-1} measuring the interaction range is displayed in Figs. 2-3. As is seen, the reduced critical temperature T_c^* sharply decreases with an the increase of the interaction range for $z^{-1} \leq 20$ and then slowly approaches the critical temperature of the RPM ($T_c^* = 0.08446$). The reduced critical density ρ_c^* demonstrates a sharp decrease in the region $z^{-1} \leq 10$ reaching the RPM critical value for $z^{-1} = 100$. A decrease of the critical temperature and the critical density expressed in the same reduced units was observed in Ref. [14].

The spinodal curves calculated from Eq. (3.3) for different values of z are shown in Fig. 4. As is seen, the spinodals change their form with the variation of the interaction range. For small values of z , the curves have a noticeable maximum at small η and change their run at higher values of η thus tending to higher temperatures. The second positive slope of spinodal curves indicates another type of the phase instability appearing in the model. When z increases, the maximum of the spinodals moves to the higher density, becomes flatter and finally disappears at $z \simeq 2.8$.

In order to calculate the coexistence curves, we use the equation (2.16) and employ the Maxwell construction. Fig. 5 shows both the co-

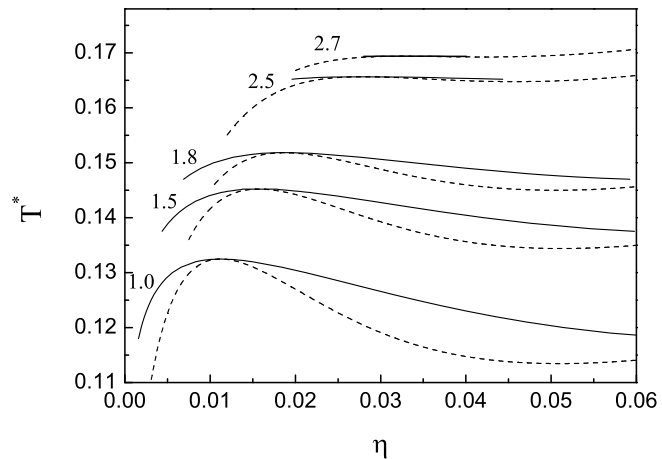


Figure 5. The coexistence curves (solid) and spinodal curves (dashed) of the YRPM for different values of z .

existence curves (solid lines) and the spinodals (dashed lines) for a set of z values. As is seen, the region of the gas-liquid coexistence in the T^* - ρ^* plane reduces with an increase of z . A disappearance of the critical point for $z < 3$ is in a qualitative agreement with the simulation study [14].

4. The crossover temperature

In order to estimate the temperature region in which the crossover from classical behavior to Ising-like critical behavior occurs, we use the Ginzburg criterion. The Ginzburg temperature expressed in terms of coefficients of the Hamiltonian (2.7) reads [19]

$$t_G = \frac{1}{32\pi^2} \frac{a_{4,0}^2}{a_{2,t} a_{2,2}^3}. \quad (4.1)$$

The relevant coefficients can be calculated using Eqs. (2.9)-(2.10), (2.13)-(2.14) and (3.1). The results for $a_{2,t}$, $a_{2,2}$ and $a_{4,0}$ and the reduced Ginzburg temperature t_G for different values of z are presented in Table 1. The dependence of the coefficients on the interaction range is shown in Figs. 6-8. While $a_{2,t}$ is a decreasing function of z^{-1} , the other two coefficients demonstrate a non-monotonous behavior. Remarkably, $a_{4,0}$ tends to zero for $z^{-1} \lesssim 0.36$ ($z \gtrsim 2.78$) indicating the presence of a

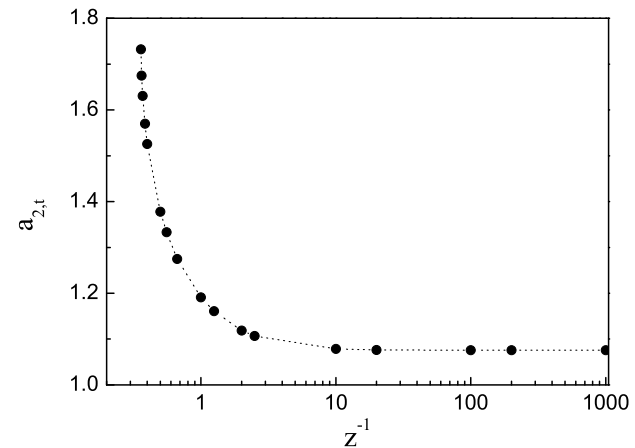


Figure 6. The coefficient $a_{2,t}$ as a function of the interaction range z^{-1} . The line is guide to the eye.

tricritical point. For $z^{-1} \geq 100$, the values of all three coefficients become equal to the values of the corresponding coefficients of the RPM [11].

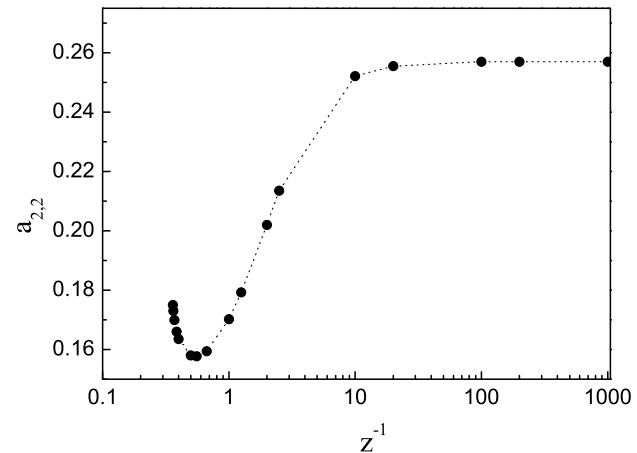


Figure 7. The coefficient $a_{2,2}$ as a function of the interaction range z^{-1} . The line is guide to the eye.

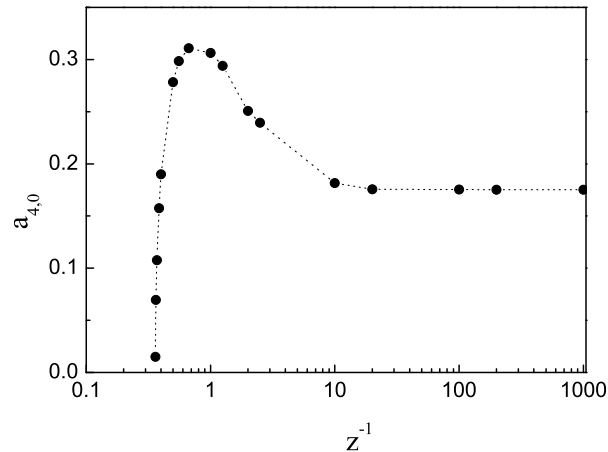


Figure 8. The coefficient $a_{4,0}$ as a function of the interaction range z^{-1} . The line is guide to the eye.

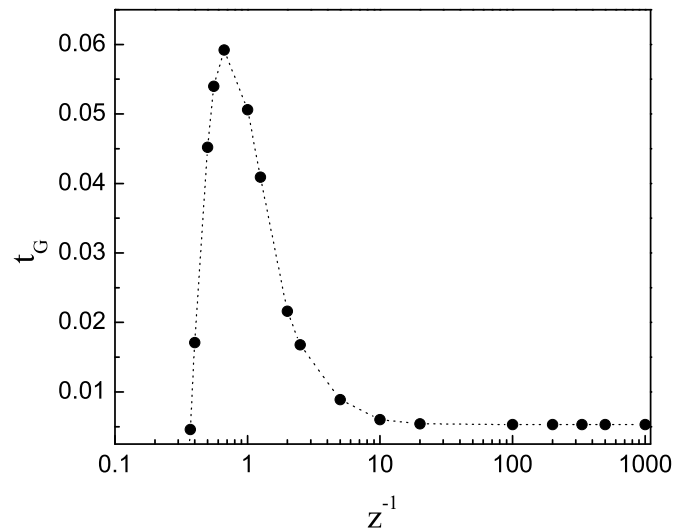


Figure 9. The reduced Ginzburg temperature as a function of the interaction range z^{-1} . The line is guide to the eye.

The dependence of the reduced Ginzburg temperature on the interaction range is shown in Fig. 9. For $z^{-1} \geq 20$, the reduced Ginzburg temperature approaches the value obtained for the RPM. For small z^{-1} , t_G shows a non-monotonous behavior passing through a maximum at $z^{-1} \simeq 0.67$ and approaching zero at $z^{-1} \lesssim 0.36$.

5. Conclusions

Using the approach that exploits the method of CVs we have studied the gas-liquid phase diagram and the crossover temperature of the screened Coulomb (Yukawa) restricted primitive model (YRPM) of oppositely charged hard spheres of diameter σ . Our results obtained within the framework of the mean-field theory have shown that the region of the gas-liquid coexistence in the plane “reduced temperature-reduced density” decreases with an increase of the inverse screening length z and completely disappears at $z \simeq 2.8$. This is in a qualitative agreement with the results of computer simulations indicating that the gas-liquid coexistence is stable for $z \leq 4$ [14].

We have studied the dependence of critical temperature and critical density on the interaction range of the Yukawa potential. With the reduced temperature defined as the inverse of the Yukawa potential contact value, the critical temperature decreases with an increase of the interaction range. The reduced critical density shows a similar trend. The both trends qualitatively agree with the results of simulations [14].

Finally, we have studied the effect of the interaction region on the crossover behavior by applying the Ginzburg criterion. Using our previous results, we have obtained explicit expressions for coefficients of the LG Hamiltonian in a one-loop approximation, and consequently calculated the Ginzburg temperature. We have shown that an increase in the interaction region leads to a decrease of the temperature region where the crossover from the mean-field critical behavior to Ising model criticality occurs. For $z^{-1} \geq 20$, the reduced Ginzburg temperature of the YRPM is the same as for the RPM.

References

1. K. Gutkowski, M.A. Anisimov, and J.V. Sengers, *J. Chem. Phys.* **114**, 3133 (2001).
2. J.V. Sengers and J.G. Shanks, *J. Stat. Phys.* **137**, 857 (2009).
3. W. Schröder, *Contrib. Plasma Phys.* **52**, 78 (2012).

4. A.-P. Hynninen and A.Z. Panagiotopoulos, *Mol. Phys.* **106**, 2039 (2008).
 5. J.-M. Caillol, D. Levesque, and J.-J. Weis, *J. Chem. Phys.* **116**, 10794 (2002).
 6. E. Luijten, M.E. Fisher, and A.Z. Panagiotopoulos, *Phys. Rev. Lett.* **88**, 185701 (2002).
 7. Y.C. Kim, M.E. Fisher, and A.Z. Panagiotopoulos, *Phys. Rev. Lett.* **95**, 195703 (2005).
 8. O.V. Patsahan and I.M. Mryglod, *J. Phys.: Condens. Matter* **16**, L235 (2004).
 9. A. Ciach, *Phys. Rev.E* **73**, 066110 (2006).
 10. A. Parola and D. Pini, *Mol. Phys.* **109**, 2989 (2011).
 11. O.V. Patsahan, *Phys. Rev. E*, **88**, 022102 (2013).
 12. M.E. Leunissen, C.G. Christova, A.P. Hynninen, C.P. Royall, A.I. Campbell, A. Imhof, M. Dijkstra, R. van Roij and A. van Blaaderen, *Nature*, **437**, 235 (2005).
 13. A.P. Hynninen, M. E. Leunissen, A. van Blaaderen and M. Dijkstra, *Phys. Rev. Lett.* **96**, 018303 (2006).
 14. A. Fortini, A.-P. Hynninen, M. Dijkstra, *J. Chem. Phys.* **125**, 094502 (2006).
 15. M. Bier, R. van Roij, M. Dijkstra, *J. Chem. Phys.* **133**, 124501 (2010).
 16. R.J.F. Leote de Carvalho, R. Evans, *Mol. Phys.* **92**, 211 (1997).
 17. J. D. Weeks, D. Chandler, and H.C. Andersen, *J. Chem. Phys.* **54**, 5237 (1971).
 18. O. Patsahan, and I. Mryglod, *Condens. Matter Phys.* **9**, 659 (2006).
 19. N. Goldenfeld, *Lectures on phase transitions and the renormalization group* (Addison-Wesley, New-York, 1992).
-

CONDENSED MATTER PHYSICS

The journal **Condensed Matter Physics** is founded in 1993 and published by Institute for Condensed Matter Physics of the National Academy of Sciences of Ukraine.

AIMS AND SCOPE: The journal **Condensed Matter Physics** contains research and review articles in the field of statistical mechanics and condensed matter theory. The main attention is paid to physics of solid, liquid and amorphous systems, phase equilibria and phase transitions, thermal, structural, electric, magnetic and optical properties of condensed matter. Condensed Matter Physics is published quarterly.

ABSTRACTED/INDEXED IN: Chemical Abstract Service, Current Contents/Physical, Chemical&Earth Sciences; ISI Science Citation Index-Expanded, ISI Alerting Services; INSPEC; "Referatyvnyj Zhurnal"; "Dzherelo".

EDITOR IN CHIEF: Ihor Yukhnovskii.

EDITORIAL BOARD: T. Arimitsu, *Tsukuba*; J.-P. Badiali, *Paris*; B. Berche, *Nancy*; T. Bryk (Associate Editor), *Lviv*; J.-M. Caillol, *Orsay*; C. von Ferber, *Coventry*; R. Folk, *Linz*; L.E. Gonzalez, *Valladolid*; D. Henderson, *Provo*; F. Hirata, *Okazaki*; Yu. Holovatch (Associate Editor), *Lviv*; M. Holovko (Associate Editor), *Lviv*; O. Ivankiv (Managing Editor), *Lviv*; Ja. Ilnytskyi (Assistant Editor), *Lviv*; N. Jakse, *Grenoble*; W. Janke, *Leipzig*; J. Jedrzejewski, *Wroclaw*; Yu. Kalyuzhnyi, *Lviv*; R. Kenna, *Coventry*; M. Korynevskii, *Lviv*; Yu. Kozitsky, *Lublin*; M. Kozlovskii, *Lviv*; O. Lavrentovich, *Kent*; M. Lebovka, *Kyiv*; R. Lemanski, *Wroclaw*; R. Levitskii, *Lviv*; V. Loktev, *Kyiv*; E. Lomba, *Madrid*; O. Makhanets, *Chernivtsi*; V. Morozov, *Moscow*; I. Mryglod (Associate Editor), *Lviv*; O. Patsahan (Assistant Editor), *Lviv*; O. Pizio, *Mexico*; N. Plakida, *Dubna*; G. Ruocco, *Rome*; A. Seitsonen, *Zürich*; S. Sharapov, *Kyiv*; Ya. Shchur, *Lviv*; A. Shvaika (Associate Editor), *Lviv*; S. Sokołowski, *Lublin*; I. Stasyuk (Associate Editor), *Lviv*; J. Strečka, *Košice*; S. Thurner, *Vienna*; M. Tokarchuk, *Lviv*; I. Vakarchuk, *Lviv*; V. Vlady, *Ljubljana*; A. Zagorodny, *Kyiv*

CONTACT INFORMATION:

Institute for Condensed Matter Physics
of the National Academy of Sciences of Ukraine
1 Svientsitskii Str., 79011 Lviv, Ukraine
Tel: +38(032)2761978; Fax: +38(032)2761158
E-mail: cmp@icmp.lviv.ua <http://www.icmp.lviv.ua>